

1 DENDRITIC SUBGLACIAL DRAINAGE SYSTEMS IN COLD GLACIERS FORMED BY  
2 CUT-AND-CLOSURE PROCESSES

3 KATHRIN NAEGELI<sup>1,2,4</sup>, HAROLD LOVELL<sup>3,4</sup>, MICHAEL ZEMP<sup>2</sup>, DOUGLAS I. BENN<sup>4,5</sup>

4

5 1 Department of Geosciences, University of Fribourg, Switzerland

6 2 Department of Geography, University of Zurich, Switzerland

7 3 School of Geography, Queen Mary University of London, United Kingdom

8 4 Arctic Geology, The University Centre in Svalbard (UNIS), Norway

9 5 School of Geography and Geosciences, University of St Andrews, United Kingdom

10

11 Naegeli K., Lovell H., Zemp M. and Benn D. I. (2014). Formation of en- and subglacial drainage systems within  
12 cold glaciers by cut-and-closure processes. *Geografiska Annaler: Series A, Physical Geography*, xx, xxx-xxx. doi:  
13 10.1111/j.1468-0459.20xx.xxxx.x

14

15 **ABSTRACT.** The routing and storage of meltwater and the configuration of drainage systems in glaciers exert a  
16 profound influence on glacier behaviour. However, little is known about the hydrological systems of cold glaciers,  
17 which form a significant proportion of the total glacier population in the climate sensitive region of the High  
18 Arctic. Using glacio-speleological techniques, we obtained direct access to explore and survey three conduit  
19 systems and one moulin within the tongue area of Tellbreen, a small cold-based valley glacier in central  
20 Spitsbergen. More than 600 m of conduits were surveyed and mapped in plan, profile and cross-section view to  
21 analyse the configuration of the drainage system. The investigations revealed that cold-based glaciers can exhibit  
22 a dendritic drainage network with supra-, en- and subglacial components formed most likely by cut-and-closure  
23 processes as well as surface-to-bed drainage via moulins. Furthermore, we observed that water is stored within the  
24 glacier and released gradually via subglacial conduits during the winter months, forming a large and active icing  
25 in the proglacial area. The presence of supra-, en- and subglacial components, the surface-to-bed moulin and the  
26 dendritic subglacial drainage network suggest that existing models and understanding of the hydrology of cold  
27 glaciers needs to be re-evaluated, mostly concerning the different possible pathways and processes that form the  
28 hydrological system.

29 *Key words:* cold glaciers, englacial/subglacial conduit, glacier hydrology, glacio-speleology, icings, Svalbard

30

31 **Introduction**

32 Determining the routing of meltwater through glacier systems is of paramount importance as the configuration of  
33 drainage networks can have a critical role to play in glacier response to meteorological forcing (cf. Hodgkins 1997)  
34 and strongly influence ice dynamics (Röthlisberger and Lang 1987; Irvine-Fynn *et al.* 2011). Both of these are  
35 important factors when considering the near-future contributions of glaciers and ice caps to the global sea level

36 budgets (Pfeffer *et al.* 2008; Radić and Hock 2011; Jacob *et al.* 2012), in addition to more local impacts such as  
37 on the hydrology of rivers and the flux of freshwater to fjord environments (Hagen *et al.* 2003).

38 The majority of studies have focused on hydrological systems within entirely temperate glaciers and, as a  
39 result, hydrological models of drainage pathways within glaciers are typically based on data from temperate  
40 glaciers only (e.g. Shreve 1972, Hooke 1989, Nienow *et al.* 1996, Fountain and Walder 1998, Mair *et al.* 2003,  
41 Fountain *et al.* 2005, Irvine-Fynn *et al.* 2011). By contrast, many glaciers in the High Arctic are either entirely  
42 cold or polythermal (Hagen *et al.* 1993) and hence do not fit into existing models of glacier hydrological processes  
43 (Gulley *et al.* 2009a; Irvine-Fynn *et al.* 2011). Furthermore, the storage and release of water throughout the winter  
44 months has typically only been observed at temperate and polythermal glaciers (Liestøl 1976; Gokhman 1987;  
45 Hagen *et al.* 2003). However, studies at Scott Turnerbreen have indicated that predominantly-cold polythermal or  
46 cold glaciers are also able to store and release water all year round (Hodgkins 1997; Hodgkins 2001; Hodgkins *et*  
47 *al.* 2004).

48 Recent developments in glacio-speleology have opened up new opportunities to make direct observations  
49 of the formation and complexity of cold and polythermal glacier drainage systems (Pulina and Rehak 1991; Vatne  
50 2001; Mavlyudov 2005; Mavlyudov 2006; Badino 2007; Gulley and Benn 2007; Benn *et al.* 2009a; Gulley *et al.*  
51 2009a). Glacio-speleological approaches have been applied in Svalbard, North America, the European Alps and  
52 the Himalaya (see Table 2 in Gulley *et al.* 2009b). This work has helped to improve our understanding of meltwater  
53 routing processes in temperate, polythermal and cold glaciers (e.g. Gulley *et al.* 2009a), conduit controls on surging  
54 (e.g. Benn *et al.* 2009b) and hydrofracturing and the formation of moulins (e.g. Benn *et al.* 2009a; Gulley *et al.*  
55 2009b). Most recently, Gulley *et al.* (2012, 2013) used surveys of a subglacial conduit below Rieperbreen,  
56 Svalbard, to evaluate conduit roughness values and the interpretation of dye-trace breakthrough curves.

57 The focus of this study is the drainage system of Tellbreen, a small valley glacier in central Spitsbergen  
58 (Fig. 1). Previous geophysical investigations on Tellbreen, the subject of this study, the glacier by Bælum and  
59 Benn (2011) indicated that the glacier is almost entirely cold based. However, a large icing forms in front of the  
60 glacier each winter, similar to Scott Turnerbreen, indicating the storage and release of substantial amounts of water  
61 within or beneath the glacier. Bælum and Benn (2011) suggested that this apparent contradiction could be  
62 explained by the presence of ‘cut-and-closure conduits’, some of which may have reached the bed. The cut-and-  
63 closure mechanism of conduit formation involves a two-stage process of channel incision by supraglacial streams  
64 followed by roof closure (Gulley *et al.* 2009a). Deep channels will form and persist wherever channel incision  
65 rates exceed glacier surface ablation rates, and roof closure can occur by snow, aufeis or breccia blockages, or wall  
66 convergence by ice creep. This is a widespread and dominant process on uncrevassed glacier surfaces in Svalbard  
67 and other cold environments, and is a plausible mechanism for forming subglacial conduits beneath thin, cold ice.  
68 Glacio-speleology provides the ideal tool to test the GPR-based conjecture of Bælum and Benn (2011), by allowing  
69 direct access to the drainage system of Tellbreen. Additionally, the analyses of supraglacial, englacial and  
70 subglacial sedimentological and glaciological structures provide further information about the formation process  
71 and temporal evolution of the drainage system and related implications.

72 The aims of this study are threefold: (1) to survey the accessible parts of the internal drainage system, (2)  
73 to test the hypothesis that subglacial drainage conduits can form by the cut-and-closure mechanism, and (3) to  
74 evaluate the extent to which such systems contribute to the routing, storage and release of water during the winter  
75 months.

76

## 77 **Study area**

78 Tellbreen is a land-terminating valley glacier situated at 78° 7' 48.00" N; 78° 7' 48.00" E in Helvetiadalen, central  
79 Spitsbergen (Fig. 1). At present, Tellbreen is ~4 km long, ~0.5 km wide, and covers an area of ~2.8 km<sup>2</sup> (Bælum  
80 and Benn 2011). The glacier ranges in elevation from ~300 m at the terminus to 950 m a.s.l., but as the tongue  
81 area has a very low gradient approximately 90% of the entire glacier surface is situated below 650 m a.s.l. (Bælum  
82 2006). From the glacier midpoint, the tongue curves towards the southeast and terminates in ~0.5 km<sup>2</sup> of ice-cored  
83 moraine. The bedrock in the area is comprised of readily erodible sandstones, siltstones and shales of the Van  
84 Mijenforden and Adventdalen Groups (Hjelle 1993; Dallmann *et al.* 2002).

85 *Ground penetrating radar* (GPR) data (Bælum 2006; Bælum and Benn 2011) indicates that the glacier is  
86 almost entirely below the pressure-melting point and therefore cold-based, except for one small and isolated area  
87 with potentially warm ice near the base of the thickest (~100 m) part of the glacier. This stands in good agreement  
88 with the general understanding of small glaciers on Svalbard having a cold thermal regime (cf. Hagen *et al.* 1993).  
89 Bælum and Benn (2011) calculated a mean ice thickness of ~50 m in 2009 and where the conduits are located on  
90 the lower tongue a maximum ice thickness of ~30 m is estimated. Crevassing is restricted to bergschrund areas  
91 and isolated open fractures on the lower tongue, which are closely associated with the cave systems investigated  
92 in this study (Fig. 1c).

93 The catchment area of Tellbreen is well defined and characterised by two accumulation basins above  
94 ~600 m a.s.l., which were the only areas with snow cover in August 2011. The equilibrium line altitude of the  
95 glacier is unknown, but as the glacier was almost entirely snow-free by August 2011 it is evident that the  
96 accumulation area is very limited (cf. Bælum and Benn 2011). The long-term mass balance of Tellbreen over the  
97 last ~100 years since *the Little Ice Age* (LIA) is calculated to be about -0.5 m w.e. yr.<sup>-1</sup> (Bælum and Benn 2011),  
98 which is consistent with the average mass balance for all Svalbard glacier of -0.55 m w.e. yr.<sup>-1</sup> (Dowdeswell *et al.*  
99 1997). During this time, Tellbreen has lost ~50% of its area and ~60% of its volume and has experienced terminus  
100 retreat of ~1 km (Bælum and Benn 2011). The flow velocity of Tellbreen during recent years is about 1.5 m yr.<sup>-1</sup>  
101 (C. Bøggild, pers.com. 2012), which can probably be almost entirely attributed to internal deformation (e.g.  
102 Etzelmüller *et al.* 2000).

103 In the proglacial area a large icing forms each winter, at least partly from water discharging from beneath  
104 the glacier (Bælum and Benn 2011). At the glacier front three meltwater conduits can be accessed (Fig. 1c),  
105 providing an insight into the hydrological system of Tellbreen. Two of them are located in debris-covered dead  
106 ice topography southwest and northeast of the clean glacier ice body (Crack and Feather caves, Fig. 1), while the  
107 third is located beneath the beneath glacier ice body (Steam cave, Fig. 1c). Crack cave is most probably connected  
108 with Steam cave and forms the main active channel feeding the proglacial icing.

109

## 110 **Methods**

111 Glacio-speleology is a relatively new and still rather rarely used approach to investigate glacier hydrological  
112 systems through the exploration of englacial and subglacial conduits in the winter months (e.g. Vatne 2001; Gulley  
113 and Benn 2007; Gulley 2009; Gulley *et al.* 2009a, 2009b), although it has a long history dating back to the 19<sup>th</sup>  
114 century (Forel 1887). In this investigation we use standard speleological techniques adapted for glacier caves

115 (Dasher 1994; Gulley and Benn 2007). All conduit systems were surveyed by producing maps and scale drawings  
116 *in situ* in plan, profile and cross-section view (cf. Gulley *et al.* 2009a).

117 The processes of glacio-speleological mapping that were applied to the three conduits located in the lower  
118 tongue (Feather, Steam and Crack caves; Fig. 1c) are described in Table 1. Feather cave was discovered and  
119 mapped in March 2011; the entrances to Steam and Crack caves and a moulin further upglacier (Fig. 1c) were  
120 located and marked in August 2011 prior to being mapped in April 2012. The three investigated conduit systems  
121 were mapped using a Leica laser rangefinder for distance measurements and Suunto compass and clinometer for  
122 the determination of the azimuth and inclination of the channels. Based on these *in situ* measurements, geometric  
123 parameters such as cave length and depth, mean slope angle and sinuosity ratio were calculated for each conduit  
124 system. The cave length and depth is the maximum height difference and length of the route any caver would  
125 travel through the cave (Dasher 1994). The overall elevation change with horizontal straight line distance (mean  
126 slope angle) and the ratio of the actual path length and the straight line length (sinuosity) help to get a better  
127 understanding of the pattern of the conduit system, i.e. whether the system is of meandering character or straight.  
128 In addition to these geometric parameters, four main morphology types based on Gulley *et al.* (2009a) are used to  
129 describe the conduit systems. *Plugged canyons* are defined as relatively narrow, tall passages, with sub-parallel  
130 walls, which are either vertical or tilted up towards the centre of meander bends, and their roofs are infilled by  
131 snow, aufeis or breccias. *Sutured canyons* are also relatively narrow and tall, but they are characterised by walls  
132 that are brought into contact by ice flow and thus do not show any infillings. *Horizontal slots* represent wide  
133 passages with low roofs, and *tubular passages* are defined as round or roughly elliptical, formed by re-enlargement  
134 of passages by wall-melting.

135 The mapping technique divides the conduit system into different sections defined by a station at each end.  
136 These stations are chosen, numbered and marked clearly to ensure an easy recovery throughout the entire mapping  
137 period. Furthermore, these stations have to be representative of their section, in order to best recreate the  
138 morphology of the conduit. At each of the stations the conduit dimensions as well as the distance, azimuth and  
139 inclination to the consecutive stations are determined, resulting in scaled drawings in plan, profile and cross-  
140 section view of the entire conduit system. The final maps presented in this paper (cf. Fig. 2, 3 and 4) were drawn  
141 using Adobe Illustrator based on the measurements and sketches taken *in situ*.

142 Finally, observations of glaciological and sedimentological features (such as glaciofluvial sediments)  
143 exposed within the conduit walls and on the glacier surface were recorded, as these can provide an insight into the  
144 origin and evolution of the drainage system (Gulley *et al.* 2009a). Clast shape and fabric data from samples of 50  
145 sandstone clasts were collected and plotted on ternary and stereographic diagrams, respectively. The  $C_{40}$  index  
146 (ratio of  $c/a$ -axis  $\leq 0.4$ ), RA (percentage of very angular and angular clasts) and RWR (percentage of well-rounded  
147 and rounded clasts) were calculated for the clast shape data following Benn and Ballantyne (1994) and Lukas *et*  
148 *al.* (2013).

149

## 150 **Results**

### 151 *Geometric parameters and morphology of conduit systems*

152 In total, 636 m of conduits were mapped in the lower tongue of Tellbreen (Fig. 1c). Within the three systems, 51  
153 stations were marked, recorded and sketched as cross-sections. The large moulin observed in the upper area of the

154 tongue was explored but not mapped to the same level of detail as the conduits. The main geometric parameters  
155 for the three conduits are shown in Table 2.

156

157 *Feather cave.* This cave system was Y-shaped consisting of a main channel (A), and a side channel (B) (Fig. 2a  
158 and 5a). The cave was mapped from southeast to northwest, i.e. upglacier from the entrance that was located at  
159  $78^{\circ} 15' 13.080''$  N;  $16^{\circ} 15' 39.960''$  E (Fig. 1c). As the cave was open on both sides, airflow through the cave was  
160 possible, forming large (15 cm) ice feathers on the cave roof (Fig. 5b). Channels A and B were 140 m and 60 m  
161 long and, with sinuosity values of 1.2 and 1.3, relatively straight. The cave descended about 7 m resulting in a  
162 moderate overall inclination (Fig. 2b). From the entrance, which consisted of a large cavern, about 20 m wide and  
163 3 m high, the channel gradually narrowed and lowered to a width of about 10 m and a height of about 1 m at station  
164 A5, located about 125 m inside the channel. The channel was incised into poorly-sorted diamict for about 50 m  
165 between station A3 and A7, interpreted as subglacial traction till (detailed discussion of the till and the overlying  
166 basal and glacier ice is provided by Lovell *et al.* (submitted). Side-channel B turned north after about 65 m from  
167 the cave entrance. This channel B was elevated by about 4.5 m and extended for 60 m before it was blocked by  
168 blown-in snow. The confluence area of channels A and B was partly filled with fallen ice blocks and at several  
169 locations daylight was visible in the roof. In general, the cross-sections of channel A were very wide and low, i.e.  
170 horizontal slots (Fig. 2a), whereas channel B displayed a tubular morphology (Figs 2a and 5j).

171

172 *Crack cave.* This cave was highly sinuous (sinuosity of 2.1) and consisted of a main channel and one small side  
173 cavity near the entrance (Fig. 3a). The entrance was located at the southwestern margin of the glacier tongue ( $78^{\circ}$   
174  $15' 8.640''$  N;  $16^{\circ} 15' 22.740''$  E; Fig. 1c) and the cave was mapped in an upglacier direction. Channel A was 145 m  
175 long and had a very low slope, with only 1 m elevation change of the cave floor over this distance (Fig. 3b). The  
176 side cavity was ~7 m by 10 m across and ~0.5 to 1 m high, and was partially blocked by wind-blown snow. Cross-  
177 sections within the first 40 m of channel A were primarily tubular in form (Fig. 5

178 c), whereas from station A5 onwards horizontal slots were more common (Fig. 5d). After 145 m the conduit  
179 dimensions were too constricted to allow further progress. The floor consisted of accumulations of aufeis with  
180 some snow in the entrance area and areas of frazil ice and ripple structures were observed further inside the cave.  
181 Shortly beyond station A6 the channel was incised into poorly-sorted diamict (subglacial till) and the floor was  
182 partly to fully covered by loose sediment and rocks (Fig. 5d).

183

184 *Steam cave.* This cave had a complex morphology and contained two confluent channels (Fig. 4a). The entrance  
185 was located at the point where a lateral supraglacial channel disappeared into the glacier ice (Fig. 5e) at the  
186 southwestern margin of the glacier tongue ( $78^{\circ} 15' 10.980''$  N;  $16^{\circ} 14' 54.780''$  E; Fig. 1c) and the cave was mapped  
187 in a downglacier direction. The system consisted of a channel aligned west-east (channel A) and a second channel  
188 B aligned northwest-southeast. This cave was the longest measured in Tellbreen, with lengths of 160 m and 80 m  
189 for channel A and B, respectively. The first approximately 50 m of channel A extending downglacier from the  
190 entrance was a relatively narrow and slightly sinuous (sinuosity of 1.3) canyon plugged by snow (cf. cross-section  
191 A7 and A8 in Fig. 4a), which widened shortly before the confluence with channel B. The ice within the floor of  
192 this confluence zone contained ripple structures. After the confluence, channel A narrowed significantly to a width

193 of only 3 m and rapidly reduced in height from 3 m at station A13 to 0.5 m at station A16. After station A16 the  
194 height of the channel increased again to about 1 to 2.5 m and extended over a length of 65 m until it divided again  
195 into two branches. One of the branches was blocked by ice blocks and debris including large boulders, and the  
196 floor of the other was too unstable to allow further investigation. The morphology of the cross-sections along  
197 channel A changed from plugged canyon at the upper end to horizontal slots at the lower end, which were always  
198 wide but varied significantly in height (0.5 to 2.6 m). In contrast, the cross-sections along channel B were all very  
199 similar, showing a high width to height ratio (e.g. Station B1, 14:3) typical for horizontal slot morphology (Fig.  
200 5f). In the upper part of this channel (from station B3 to B4) the floor was covered by large ice blocks and debris  
201 and at the upglacier extent the channel appeared to have been squeezed shut (cf. Gulley *et al.* 2009a). In the  
202 uppermost 16 m of channel A, the conduit floor is very steep, with an elevation change of about 8 m. Below this,  
203 the entire system is gently sloping, demonstrated by the mean slope angle of 0.130 for the entire length of channel  
204 A and 0.026 for channel B (Fig. 4b). Both channels were incised into poorly-sorted diamict (subglacial till), except  
205 for the upper steep part below the entrance. The cave floor was covered by wind-blown snow until station A10,  
206 but also contained frazil ice, ripple structures and loose sediment.

207

208 *Moulin.* The moulin (Fig. 1c) is located on the northern side of the lower glacier tongue approximately 1.2 km  
209 upglacier from the terminus (78° 15' 26.460" N; 16° 13' 47.640" E; Fig. 1c). The upper 10 m of the moulin  
210 consisted of a narrow, ~1.5 m wide bottleneck, after which it opened up to form a 32 m high and 16 m wide dome-  
211 shaped hall. From the base of the moulin, a very large (8 m wide and 12 m high) N-channel extending downglacier  
212 was incised into the sediment and underlying bedrock (Fig. 5g), showing that the moulin connects the glacier  
213 surface directly to the bed. A very narrow (0.8 m wide) channel extended upglacier from the base of the moulin,  
214 but was blocked by snow after a few meters. The roof of this passage consisted of two separate ice walls that are  
215 in contact (Fig. 5i). The N-channel transitioned into a small (1 m wide and 0.5 m high) R-channel after about 80 m,  
216 which continued for approximately 7 m before it was blocked by boulders and gravel (Fig. 5h).

217

#### 218 *Glaciological features*

219 Several unique glaciostructural features were identified within the caves. The flat, disk shaped bubble structure  
220 shown in Fig. 6b was observed in all caves, but mainly in the tubular part of Crack cave. These bubbles were  
221 horizontally-aligned, easily visible in the clear ice and ranged from few centimetres up to 0.5 m in diameter.  
222 Usually, they were observed in small groups in the conduit roofs, walls and floors. Ripple structures were found  
223 within the floors of all caves (Fig. 6d). They extended over distances of few decimetres up to few meters, where  
224 the floors showed greater slope angles of around 5°. The ripples observed in Crack cave contained frazil ice,  
225 whereas others consisted of clear ice. Icicles were found in several places in the conduit systems, such as the one  
226 shown in Fig. 6a located between stations A7 and A8 in Crack cave (cf. Fig. 3a). This example bridged between  
227 cave roof and floor, covering a height of 0.73 m, and was deformed but showed no fractures. Measured along its  
228 length, the icicle is 4 cm longer than the straight-line distance between roof and floor, indicating that the roof was  
229 very slowly closing down after the formation of the icicle at the end of the previous ablation season. Icicles which  
230 did not extend the full distance to the cave floor were also commonly observed (Fig. 6c).

231

232 *Sedimentological features and characteristics*

233 In several places bands of sorted sediment were exposed in the walls of the conduit systems and at the glacier  
234 surface. The englacial exposures primarily consist of sorted sand and gravel, which range in thickness from ~2  
235 to 150 cm and can extend laterally for up to 15 m (Fig. 6e, h). Figure 7a shows such an exposure in the entrance  
236 cavern of Feather cave (Fig. 2a). Here, a ~2 m-thick layer of poorly-sorted diamict and the overlying glacier ice  
237 cross-cut by layers of sorted fine sand, interbedded sands and gravels and clast-supported massive gravel. The  
238 diamict and basal ice sequence are described in detail by Lovell *et al.* (submitted) and are not considered further  
239 here. The sorted fine sand layers, which range from 10 to 50 cm in thickness, display small laminations, which in  
240 places record small-scale folding. These layers are overlain by interbedded coarse sands and fine gravels which  
241 dip down channel at ~30° towards the left-hand (downglacier) end of the exposure. Clast-supported coarse gravel  
242 layers are also present, the largest of which is ~50 cm thick and extends for ~6 m. The clasts within these are  
243 predominantly sub-angular to sub-rounded (Fig. 7b) and are imbricated, with an orientation of ~000-040° (Fig.  
244 7c). The sediment band cuts across glaciological structures such as foliation and old crevasse traces, showing that  
245 they post-date deformation of the ice. Similar assemblages of sediments were found in debris bands within all  
246 caves, some of which extended laterally for several metres along the sidewalls, e.g. in channel B of Feather cave  
247 (cf. Fig. 5j). In several places, there are paired debris bands of similar character on opposite walls. In some cases,  
248 debris bands can be shown to occupy sutures, where the cave roof and floor have been brought into contact by ice  
249 creep. An example between stations A6 and A7 of Crack cave is shown in Figure 5k. At this site, the cave floor  
250 consists of a series of sand and gravel covered terraces, recording vertical and lateral incision of the channel  
251 through glacier ice to the bed (top left to bottom right in the photograph). The uppermost terrace is capped by  
252 bedded, well-sorted sand, the upper surface of which is in contact with the gently sloping cave roof. This contact  
253 can be traced laterally up-channel to a series of narrow, open voids between cave floor and roof, and down-channel  
254 to sediment layers cutting across the glacier ice, similar to those observed elsewhere.

255 In August 2011, small (~0.5 m high) piles of coarse sand and fine gravel were observed on the glacier  
256 surface (Fig. 6f, g). These were typically located immediately adjacent to incised supraglacial channels in the  
257 upglacier part of the lower glacier tongue. The piles were also observed below the glacier surface on shelves within  
258 the channel walls and in englacial positions.

259

260 **Discussion**

261 *Cut-and-closure channel origin*

262 All three mapped cave systems have englacial and subglacial sections. For example, in Feather cave channel B is  
263 entirely located within glacier ice, whereas exposures of basal till occur along much of channel A. Steam cave  
264 extends downglacier from a supraglacial channel, into an englacial section with a roof consisting of snow and ice  
265 breccia plugs, and finally to subglacial reaches where the channel has incised into basal till. This demonstrates the  
266 presence of a surface-fed englacial and subglacial drainage network, as suggested by Bælum and Benn (2011)  
267 based on GPR data.

268 The bands of sorted sediments exposed in the walls of all three caves are interpreted as suture infills of glaciofluvial  
269 material, where cave roofs came into contact with former channel floors, sealing off the upper, older levels of the  
270 system. This is most clearly demonstrated in the reach of Crack cave shown in Figure 5k. In the other caves, the

271 cross-cutting relationship between the sediment bands and glaciological structures such as ice foliation supports  
272 the conclusion that all the subglacial reaches formed by the process of cut-and-closure.

273 Altogether, these observations provide strong evidence that the three conduit systems were formed by a  
274 cut-and-closure process, in which supraglacial channels progressively developed into plugged canyons with roofs  
275 of snow and aufeis, then sutured canyons closed by ice creep, and finally to horizontal slots and N-channels at the  
276 glacier bed with sediment-filled sutures at their lateral margins. Furthermore, the moulin clearly shows that surface  
277 to bed drainage is possible in cold ice.

278 The roof of the large channel extending downglacier from the bottom of the moulin consists of glacier ice and the  
279 floor was deeply incised into the glacier bed. Moreover, the roof showed a clear suture line (Fig. 5i), which formed  
280 when two ice walls squeezed together due to ice flow. We therefore infer that this large N-channel also evolved  
281 from a former incised supraglacial channel.

282 The branching planforms of both Feather and Steam caves provides the first evidence for dendritic channel  
283 systems at the bed of cold glaciers. All other recorded cases of subglacial channels below small glaciers in Svalbard  
284 consist of single, unbranching conduits (e.g. Longyearbreen: Humlum *et al.* 2005, van Hoof 2008; Scott  
285 Turnerbreen: Temminghoff 2009; and Rieperbreen: Gulley *et al.* 2012, 2013). The existence of dendritic subglacial  
286 channel networks, which likely evolved from branching supraglacial channels, suggests that surface water may be  
287 able to access significant parts of the bed of cold glaciers, at least where the ice is thin.

288

#### 289 *Water flow and storage within the drainage system*

290 Bælum and Benn (2011) interpreted localized GPR reflections as evidence of water below the lower glacier tongue  
291 of Tellbreen and hypothesised that this water was restricted to discrete channels. They concluded that warm-based  
292 conditions were not necessary for the presence of water flow beneath glaciers in the winter months and, therefore,  
293 that subglacial water storage cannot be directly linked to subglacial water production. This is supported by the  
294 observations of our study, in which water flow was clearly audible in April 2012 and also visible in the form of  
295 wet and slushy cave floors. Furthermore, most of the ice-floored channels consisted of refrozen meltwater, often  
296 containing frozen ripple structures, rather than glacier ice, which typically takes the form of intercalated layers of  
297 bubble-rich and bubble-poor ice (cf. Hubbard *et al.* 2000).

298 The different morphologies of the channels provide information about the water level in the past. Tubular  
299 channel shapes, as observed in the lowermost 40 m of Crack cave and the full length of channel B in Feather cave,  
300 form under constricted, transient phreatic (epiphreatic; Gulley *et al.* 2009a) conditions during periods of high  
301 meltwater discharge, when channels are enlarged by wall melting. Pipe-full discharge therefore occurred at some  
302 point in the formation of these caves. In addition, the disk-like bubble structures, mostly observed within sections  
303 with a tubular morphology, most probably form under phreatic (pipe-full; Gulley *et al.* 2009a) conditions, when  
304 dissolved gases accumulate during the slow freezing of the ice, forming gas occlusions (Lorrain *et al.* 2002;  
305 Boereboom *et al.* 2012).

306 Figure 8 illustrates the water pathways observed in Tellbreen as a conceptual model showing the suggested  
307 evolution of the hydrological system of cold valley glaciers on Svalbard. The model stages (a)-(f) present both  
308 temporal and spatial evolution of the drainage system. Stage (a) shows a section of a glacier located in the upper  
309 tongue area. Meltwater in this area is mainly routed within supraglacial channels. As discharges increase



310 downglacier, incision rates exceed ablation rates in the adjacent ice, leading to progressive channel deepening  
311 (Gulley *et al.* 2009a). Former bedload of the stream can be stored in upper, abandoned levels of the channels, and  
312 later melt out forming piles of glaciofluvial sediments on the glacier surface (stage (d) and (e); cf. Fig. 6f, g). In  
313 addition, moulins can be present that route meltwater directly from the surface to the glacier bed.

314 The supraglacial channel in stage (a) is still fully open, and stage (b) indicates the progressive plugging by  
315 snow, aufeis and ice breccias created by collapses (Gulley *et al.* 2009a). In stage (c), the channel is already partly-  
316 closed and plugging continues at the glacier surface. Further downglacier, but also at a later time-step, this partly-  
317 closed channel is completely disconnected from the surface and is a fully englacial channel (stage (d)). In addition,  
318 abandoned meander fills can be observed on the glacier surface from the earlier active supraglacial channel. In the  
319 lower tongue, these englacial channels usually incise down to the glacier bed. Here, the meltwater can either erode  
320 into subglacial sediments or bedrock, i.e. a N-channel (stage (e)), or be incised up into the ice, i.e. a R-channel  
321 (stage (f)). The dendritic form of the subglacial channel network is inherited from former confluent supraglacial  
322 streams. Stage (f) also shows the proglacial area, including streams exiting the glacier through portals and, in  
323 winter months, forming proglacial icings.

324

#### 325 *Implications for existing glacier hydrological theories*

326 Many glacier hydrological studies have focused on topics such as meltwater flow over different types of beds (e.g.  
327 Röthlisberger 1972; Kamb 1987; Walder and Fowler 1994) or pathways and routing of meltwater within and  
328 beneath the ice body (e.g. Tranter *et al.* 1996; Fountain and Walder 1998; Fountain *et al.* 2005). Many conceptual  
329 models are largely based only on temperate glaciers, and, to a lesser extent, polythermal glaciers (Gulle, *et al.*  
330 2009b; Irvine-Fynn *et al.* 2011). Comparable studies of cold glaciers are, however, almost completely lacking.  
331 Nevertheless, in recent years new conceptual ideas have arisen about water routing in glacier ice and it is now  
332 widely recognized that hydrofracturing (e.g. Boon and Sharp 2003; Benn *et al.* 2009a) and the exploitation of  
333 permeable structures (e.g. Gulley *et al.* 2009b) are efficient processes that are able to route water through cold ice.  
334 Furthermore, the process of cut-and-closure has been observed on glaciers with partly or entirely cold ice, and this  
335 is therefore a third mechanism that is capable of creating supra- en- and subglacial drainage networks in cold  
336 glaciers (Gulley *et al.* 2009a). This latter mechanism is strongly supported by the observations at Tellbreen. There  
337 is no evidence that any of the drainage systems we have observed have evolved from relict ‘Shreve-type’ conduits,  
338 formed normal to equipotential surfaces in permeable temperate ice (Shreve, 1972) as suggested in some previous  
339 studies (Hodgkins 1997; Stuart *et al.* 2003).

340 Moreover, drainage systems within cold glaciers were conventionally suggested to have a simple  
341 configuration, as drainage was assumed to be restricted to surface runoff (cf. Hodgkins 1997). The evidence from  
342 Tellbreen demonstrates that the conduit drainage system within cold glaciers can in fact be dendritic, reflecting  
343 the temporal and spatial evolution of channels through cut-and-closure processes.

344 Icings form by the refreezing of gradually released meltwater throughout the winter months (Irvine-Fynn  
345 *et al.* 2011) and were for a long time believed to be a clear indicator of a polythermal regime of the glacier (Liestøl  
346 1976; Gokhman 1987; Hagen *et al.* 2003). More recent studies conducted at Scott Turnerbreen (Hodgkins 2001;  
347 Hodgkins *et al.* 2004), a similar-sized valley glacier to Tellbreen and also consisting of predominantly cold ice,  
348 questioned this strict link between icings and temperate or polythermal glaciers, although the question as to how  
349 water could be stored within cold glaciers remained unanswered. The detailed investigations of the three conduits

350 systems in the lower tongue and the presence of a large and active icing in the front of Tellbreen during April  
351 demonstrate that water stored beneath Tellbreen can be released during the winter months via subglacial conduits.  
352 The origin of this water, however, remains unknown.

353 The fact that a cold-based glacier like Tellbreen apparently experiences year round water storage and flux  
354 also implies that the erosional capability and solute flux below cold glaciers such as Tellbreen is greater than  
355 previously assumed. As seen from this study, cold glaciers may be capable of storing and releasing water year  
356 round and should therefore be considered as an active component in the hydrological cycle and its seasonal  
357 distribution and response to meteorological forcing.

358

### 359 **Conclusions**

360 The systematic glacio-speleological investigation of three conduit systems and a moulin in the tongue area of  
361 Tellbreen, an almost entirely cold glacier in Svalbard, provide an insight into the hydrological systems of cold-  
362 based valley glaciers. This shows that:

- 363 • Glacio-speleology is a powerful technique to improve the understanding of glacier hydrology and enables the  
364 exploration of englacial and subglacial components of the drainage system.
- 365 • The drainage systems of cold valley glaciers can be dendritic and have supra-, en- and subglacial components.  
366 Water can also be routed directly from the glacier surface to the bed via moulins.
- 367 • Cut-and-closure is an effective process for forming drainage systems within cold glaciers and results in a  
368 transition from supraglacial channels in the upper ablation area to englacial and subglacial channels in the  
369 lower ablation area.
- 370 • Proglacial icings in front of cold glaciers can be directly linked to water released from the glacier and  
371 transported via subglacial channels.

372 The observations and results presented in this paper suggest that current concepts about glacier drainage systems  
373 in cold glaciers need re-evaluation, specifically concerning the different possible pathways, processes forming the  
374 conduits and capability of storing and releasing water, and reveals that further investigations of meltwater  
375 pathways, storage and release in cold glaciers are required in order to improve our current understanding.

376

### 377 **Acknowledgements**

378 KN was funded by an Arctic Field Grant from the Research Council of Norway, the Swiss Society for Speleology  
379 and the travel grant commission of the Swiss Academy of Science. HL was funded by a NERC PhD studentship  
380 (NE/I528050/1), the Queen Mary Postgraduate Research Fund and an Arctic Field Grant from the Research  
381 Council of Norway. Landsat satellite images were provided by USGS Earth Explorer and aerial photographs were  
382 acquired from the Norsk Polarinstitut. Fieldwork support from the Logistics Department of the University Centre  
383 in Svalbard was vital and we are grateful to E. Fleming, B. Hubbard, N. Hulton and Ph. Schuppli for their  
384 contributions to the collection of field data, and to all members of AG-325 in 2011, who were present when the  
385 cave systems of Tellbreen were first discovered. The photograph reproduced in Figure 5k was taken by E. Welty.

386 We thank W. Haeberli for the stimulating discussion of the glaciological features and M. Huss, L. Sold, M. Fischer  
387 and two anonymous reviewers for their detailed and thoughtful manuscript review.

388

389 *Kathrin Naegeli, Department of Geosciences, University of Fribourg, Chemin de Musée 4, 1700 Fribourg,*  
390 *Switzerland.*

391 *Email: [kathrin.naegeli@unifr.ch](mailto:kathrin.naegeli@unifr.ch)*

392 *Harold Lovell, Department of Geography, University of Portsmouth, Buckingham Building, Lion Terrace,*  
393 *Portsmouth, PO1 3HE, UK.*

394 *Email: [harold.lovell@port.ac.uk](mailto:harold.lovell@port.ac.uk)*

395 *Michael Zemp, Department of Geography, University of Zurich – Irchel, Winterthurerstrasse 190, 8057 Zürich,*  
396 *Switzerland.*

397 *Email: [michael.zemp@geo.uzh.ch](mailto:michael.zemp@geo.uzh.ch)*

398 *Douglas I. Benn, Arctic Geology, The University Centre in Svalbard (UNIS), P.O. Box 156, N-9171 Longyearbyen,*  
399 *Norway.*

400 *Email: [doug.benn@unis.no](mailto:doug.benn@unis.no)*

401

## 402 **References**

- 403 Badino, G., 2007. *Caves of Sky: A Journey into the Heart of Glaciers*. Graffice Tintoretto, Italy, 154 pp.
- 404 Bælum, K., 2006. *Mapping of the general shape, depth and various internal structures of Tellbreen, a glacier on*  
405 *Svalbard, by means of GPR (Ground Penetrating Radar)*. MS diss., Department of Geoscience, University  
406 *of Aarhus, Denmark.*
- 407 Bælum, K. and Benn, D.I., 2011. Thermal structure and drainage system of a small valley glacier (Tellbreen,  
408 Svalbard), investigated by ground penetrating radar. *The Cryosphere*, 5, 139–149. doi:10.5194/tc-5-139-  
409 2011
- 410 Benn, D.I., Gulley, J.D., Luckman, A., Adamek, A. and Glowacki, P. S., 2009a. Englacial drainage systems  
411 formed by hydrologically driven crevasse propagation. *Journal of Glaciology*, 55 (191), 513–523. doi:  
412 10.3189/002214309788816669
- 413 Benn, D.I. and Ballantyne, C.K., 1994. Reconstructing the transport history of glacial sediments: a new  
414 approach based on the co-variance of clast form indices. *Sedimentary Geology*, 91, 215–227. doi:  
415 10.1016/0037-0738(94)90130-9
- 416 Benn, D.I., Kristensen, L. and Gulley, J.D., 2009b. Surge propagation constrained by a persistent subglacial  
417 conduit, Bakaninbreen – Paulabreen, Svalbard. *Annals of Glaciology*, 50 (52), 81–86. doi:  
418 10.3189/172756409789624337
- 419 Boereboom, T., Depoorter, M., Coppens, S. and Tison, J.-L., 2012. Gas properties of winter lake ice in Northern  
420 Sweden: implication for carbon gas release. *Biogeosciences*, 9, 827–838. doi:10.5194/bg-9-827-2012
- 421 Boon, S. and Sharp, M., 2003. The role of hydrologically-driven ice fracture in drainage system evolution on an  
422 Arctic glacier. *Geophysical Research Letters*, 30 (18), 1–4. doi:10.1029/2003GL018034
- 423 Dallmann, W.K., Ohta, Y., Elvevold, S. and Blomeier, D., 2002. *Bedrock map of Svalbard and Jan Mayen,*  
424 *Norsk Polarinstittutt Temakart No. 33.*
- 425 Dasher, G.R., 1994. *On Station*, Huntsville: National Speleological Society, Inc.
- 426 Dowdeswell, J.A., Hagen, J.O., Björnsson, H., Glazovsky, A.F., Harrison, W.D., Holmlund, P., Jania, J.,  
427 Koerner, R.M., Lefauconnier, B., Ommanney, C.S.L. and Thomas, R.H., 1997. The mass balance of  
428 circum-Arctic glaciers and recent climate change. *Quaternary Research*, 48, 1–14.  
429 doi:10.1006/qres.1997.1900
- 430 Etzelmüller, B., Ødegård, R.S., Vatne, G., Mysterud, R.S. and Sollid, J.L., 2000. Glacier characteristics and  
431 sediment transfer system of Longyearbreen and Larsbreen, western Spitsbergen. *Norwegian Journal of*  
432 *Geography*, 54 (4), 157–168. doi: 10.1080/002919500448530
- 433 Forel, M.F.-A., 1887. La grotte naturelle du glacier d’Arolla. *Archives des sciences physiques et naturelles*.

434 Fountain, A.G., Jacobel, R.W., Schlichting, R. and Jansson, P., 2005. Fractures as the main pathways of water  
435 flow in temperate glaciers. *Nature*, 433 (7026), 618–21. doi:10.1038/nature03296

436 Fountain, A.G. and Walder, J.S., 1998. Water flow through temperate glaciers. *Reviews of Geophysics*, 36, 299–  
437 328. doi:10.1029/97RG03579

438 Gokhman, V.V., 1987. Distribution and conditions of formation of glacial icings on Spitsbergen. *Polar  
439 Geography and Geology*, 11 (4), 249–260. doi: 10.1080/10889378709377334

440 Gulley, J.D., Benn, D.I., Müller, D. and Luckman, A., 2009a. A cut-and-closure origin for englacial conduits in  
441 uncrevassed regions of polythermal glaciers. *Journal of Glaciology*, 55 (189), 66–80. doi:  
442 10.3189/002214309788608930

443 Gulley, J.D., Walthard, P., Martin, J., Banwell, A.F., Benn, D.I. and Catania, G., 2012. Conduit roughness and  
444 dye-trace breakthrough curves: why slow velocity and high dispersivity may not reflect flow in distributed  
445 systems. *Journal of Glaciology*, 58 (211), 915–925. doi: 10.3189/2012JoG11J115

446 Gulley, J.D., Spellman, P.D., Covington, M.D., Martin, J.B., Benn, D.I. and Catania, G., 2013. Large values of  
447 hydraulic roughness in subglacial conduits during conduit enlargement: implications for modeling conduit  
448 evolution. *Earth Surface Processes and Landforms*, 39 (3), 296–310. doi: 10.1002/esp.3447

449 Gulley, J.D., Benn, D.I., Screaton, E. and Martin, J., 2009b. Mechanisms of englacial conduit formation and  
450 their implications for subglacial recharge. *Quaternary Science Reviews*, 28, 1984–1999.  
451 doi:10.1016/j.quascirev.2009.04.002

452 Gulley, J.D., 2009. Structural control of englacial conduits in the temperate Matanuska Glacier, Alaska, USA.  
453 *Journal of Glaciology*, 55 (192), 681–690. doi: 10.3189/002214309789470860

454 Gulley, J.D. and Benn, D.I., 2007. Structural control of englacial drainage systems in Himalayan debris-covered  
455 glaciers. *Journal of Glaciology*, 53 (182), 399–412. doi: 10.3189/002214307783258378

456 Hagen, J.O., Liestøl, O., Roland, E. and Jørgensen, T., 1993. *Glacier atlas of Svalbard and Jan Mayen*, Oslo:  
457 Meddelelser Nr. 129 Norsk Polar Institutt.

458 Hagen, J.O., Kohler, J., Melvold, K. and Winther, J.-G., 2003. Glaciers in Svalbard: mass balance, runoff and  
459 freshwater flux. *Polar Research*, 22 (2), 145–159.

460 Hjelle, A., 1993. *Geology of Svalbard*, Oslo: Norsk Polarinstitut.

461 Hodgkins, R., 1997. Glacier hydrology in Svalbard, norwegian high arctic. *Quaternary Science Reviews*, 16,  
462 957–973. doi: 10.1016/S0277-3791(97)00032-2

463 Hodgkins, R., 2001. Seasonal evolution of meltwater generation, storage and discharge at a non-temperate  
464 glacier in Svalbard. *Hydrological Processes*, 15, 441–460. doi: 10.1002/hyp.160

465 Hodgkins, R., Tranter, M. and Dowdeswell, J.A., 2004. The characteristics and formation of a High-Arctic  
466 proglacial icing. *Geografiska Annaler: Series A, Physical Geography*, 86 (3), 265–275. doi:  
467 10.1111/j.0435-3676.2004.00230.x

468 Hooke, R.L., 1989. Englacial and subglacial hydrology: A qualitative review. *Arctic and Alpine Research*, 21  
469 (3), 221–233.

470 Hubbard, B., Tison, J.-L., Janssens, L. and Spir, B., 2000. Ice-core evidence of the thickness and character of  
471 clear facies basal ice: Glacier de Tsanfleuron, Switzerland. *Journal of Glaciology*, 46 (152), 140–150. doi:  
472 10.3189/172756500781833250

473 Irvine-Fynn, T.D.L., Hodson, A.J., Moorman, B.J., Vatne, G. and Hubbard, A.L., 2011. Polythermal glacier  
474 hydrology: A review. *Reviews of Geophysics*, 49 (RG4002), 1–37. doi:10.1029/2010RG000350

475 Jacob, T., Wahr, J., Pfeffer, T.W. and Swenson, S., 2012. Recent contributions of glaciers and ice caps to sea  
476 level rise. *Nature*, 482 (7386), 514–518. doi:10.1038/nature10847

477 Kamb, B., 1987. Glacier surge mechanism based on linked cavity configuration of the basal water conduit  
478 system. *Journal of Geophysical Research*, 92 (B9), 9083–9100. doi: 10.1029/JB092iB09p09083

479 Liestøl, O., 1976. Pings, springs, and permafrost in Spitsbergen. In *Norsk Polarinstitut Årbok*. 7–29.

480 Lorrain, R., Sleewaegen, S. and Fitzsimons, S., 2002. Ice formation in an Antarctic glacier-dammed lake and  
481 implications for glacier-lake interactions. *Arctic, Antarctic, and Alpine Research*, 34 (2), 150–158. doi:  
482 10.2307/1552466

483 Lovell, H., Fleming, E.J., Benn, D.I., Hubbard, B., Lukas, S. and Naegeli, K., submitted. Former dynamic  
484 behaviour of a cold-based valley glacier on Svalbard revealed by structural glaciology and basal ice  
485 investigations. *Journal of Glaciology*.

486 Lukas, S., Benn, D.I., Boston, C.M., Brook, M., Coray, S., Evans, D.J.A., Graf, A., Kellerer-Pirklbauer, A.,  
487 Kirkbride, M.P., Krabbendam, M., Lovell, H., Machiedo, M., Mills, S.C., Nye, K., Reinardy, B.T.I., Ross,  
488 F.H. and Signer, M., 2013. Clast shape analysis and clast transport paths in glacial environments: A critical  
489 review of methods and the role of lithology. *Earth-Science Reviews*, 121, 96–116. doi:  
490 10.1016/j.earscirev.2013.02.005

491 Mair, D., Willis, I., Fischer, U.H., Hubbard, B., Nienow, P., Hubbard, A., 2003. Hydrological controls on  
492 patterns of surface, internal and basal motion during three spring events': Haut Glacier d'Arolla,  
493 Switzerland. *Journal of Glaciology*, 49 (167), 555–567. doi: 10.3189/172756503781830467

494 Mavlyudov, B.R., 2005. About new type of subglacial channels, Spitsbergen. In Mavlyudov, B.R. (ed.), *Glacier*  
495 *Cave and Glacial Karst in High Mountains and Polar Regions*. Moscow: Institute of Geography of the  
496 Russian Academy of Sciences, 54–60.

497 Mavlyudov, B.R., 2006. *Internal drainage systems of glaciers* (in Russian), Moscow, 395 pp.

498 Nienow, P., Sharp, M. and Willis, I., 1996. Temporal switching between englacial and subglacial drainage  
499 pathways: dye tracer evidence from the Haut Glacier d’Arolla, Switzerland. *Geografiska Annaler: Series*  
500 *A, Physical Geography*, 78 (1), 51–60. doi: 10.2307/521134

501 Pfeffer, T.W., Harper, J.T. and O’Neel, S., 2008. Kinematic constraints on glacier contributions to 21st-century  
502 sea-level rise. *Science*, 321, 1340–3. doi: 10.1126/science.1159099

503 Pulina, M. and Rehak, J., 1991. Glacier caves in Spitsbergen. In Eraso, A., (ed.) *1st International Symposium of*  
504 *Glacier Caves and Karst in Polar Regions*. Madrid, 93–117.

505 Radić, V. and Hock, R., 2011. Regionally differentiated contribution of mountain glaciers and ice caps to future  
506 sea-level rise. *Nature Geoscience*, 4 (2), 91–94. doi: 10.1038/NGEO1052

507 Röthlisberger, H., 1972. Water pressure in intra- and subglacial channels. *Journal of Glaciology*, 11 (62), 7–13.

508 Röthlisberger, H. and Lang, H., 1987. Glacial hydrology. In Gurnell, A.M. and Clark, M.J., (eds), *Glacio-fluvial*  
509 *sediment transfer: An alpine perspective*. Chichester, West Sussex: John Wiley & Sons Ltd, 37–44.

510 Shreve, R.L., 1972. Movement of water in glaciers. *Journal of Glaciology*, 11 (62), 205–214.

511 Stuart, G., Murray, T., Gamble, N., Hayes, K. and Hodson, A.J., 2003. Characterization of englacial channels by  
512 ground-penetrating radar: An example from Austre Brøggerbreen, Svalbard. *Journal of Geophysical*  
513 *Research*, 108 (B11), 1–13. doi:10.1029/2003JB002435

514 Tranter, M., Brown, G.H., Hodson, A.J. and Gurnell, A.M., 1996. Hydrochemistry as an indicator of subglacial  
515 drainage system structure: a comparison of alpine and sub-polar environments. *Hydrological Processes*,  
516 10, 541–556.

517 Vatne, G., 2001. Geometry of englacial water conduits, Austre Brøggerbreen, Svalbard. *Norwegian Journal of*  
518 *Geography*, 55 (2), 85–93. : doi: 10.1080/713786833

519 Walder, J.S. and Fowler, A., 1994. Channelized subglacial drainage over a deformable bed. *Journal of*  
520 *Glaciology*, 40 (134), 3–15.

521

522 Manuscript received 20 Dec., 2013, revised and accepted 16 Jun., 2014

523

524 **Table 1.** Glacio-speleological mapping procedure.

Stage	Task
1	Find potential cave entrances during ablation season, e.g. where supraglacial meltwater channels disappear below the glacier surface.
2	Identify entrances and explore caves during accumulation season. Important: Always consider safety – be aware of meltwater, instabilities in the ice, instable snow plugging, etc.
3	Cave mapping: scaled dimensions
	<i>Define stations which are:</i>
3.1	<ul style="list-style-type: none"> <li>▪ <i>representative for a section of the passage</i></li> <li>▪ <i>a maximum of 20 m apart from each other</i></li> <li>▪ <i>visible from both adjacent stations</i></li> </ul>
	<i>Measurements between two consecutive stations:</i>
3.2	<ul style="list-style-type: none"> <li>▪ <i>distance</i></li> <li>▪ <i>azimuth</i></li> <li>▪ <i>inclination</i></li> </ul>
	<i>Measurements at each station:</i>
	<ul style="list-style-type: none"> <li>▪ <i>Dimensions of the passage at that point (up/down (height) and left/right (width))</i></li> </ul>
4	Cave mapping: detailed plan, profile and cross-sections view
4.1	<i>Sketch the outlines to get a plan and a profile view map</i>
4.2	<i>Include observed features in the plan-view map (e.g. snow, icicles, floor ice structures, rocks, etc.)</i>
4.3	<i>Sketch cross-sections at each station including observed features (see 4.2)</i>
5	Complete map
	<i>Draw plan, profile and cross-section view maps including all recorded details</i>
	<i>Calculate geometric parameters:</i>
6	<ul style="list-style-type: none"> <li>▪ <i>Cave length</i></li> <li>▪ <i>Cave depth</i></li> <li>▪ <i>Straight line length</i></li> <li>▪ <i>Mean slope angle</i></li> <li>▪ <i>Sinuosity ratio</i></li> </ul>
7	Application of additional methods <i>e.g. ice sampling for isotopic analysis, glacio-structural measurements, etc.</i>

525

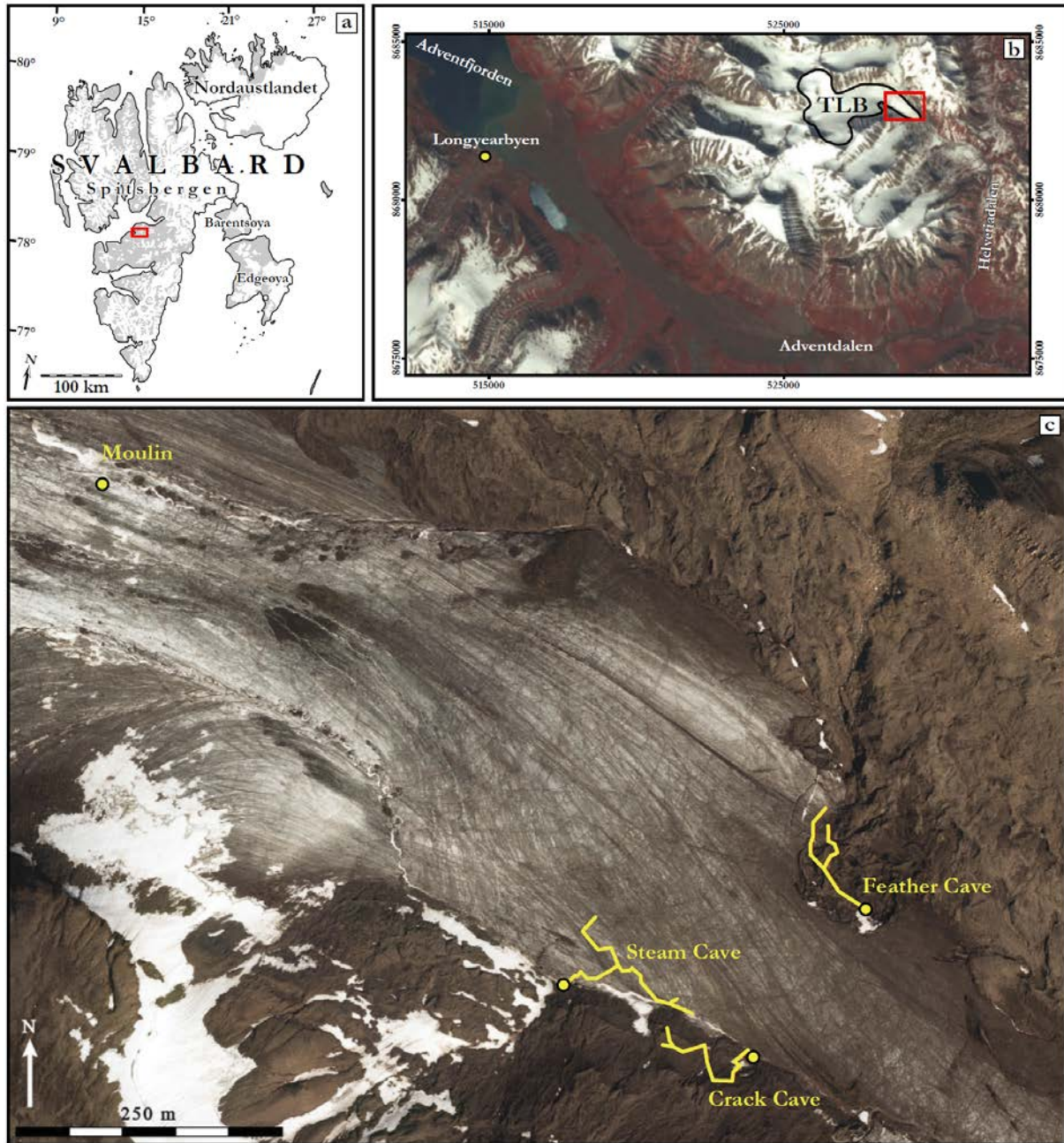
526

527 **Table 2.** Geometric parameters for the three investigated cave systems in the lower tongue (see Fig. 1c for  
 528 locations).

Geometric Parameter	Feather cave		Crack cave		Steam cave	
	Conduit Part	Conduit Part	Conduit Part	Conduit Part	Conduit Part	Conduit Part
	A (Stations A1- A8)	B (Stations A3- B7)	A (Stations A1- End)	B (Stations A4- B2)	A (Stations A1- End1)	B (Stations A11- B_End)
Number of Stations	8	7	12	2	18	4
Channel Length (m)	139.0	57.7	145.2	19.6	157.5	79.9
Straight Line Length (m)	115.5	45.5	69.0	10.0	125.0	54.0
Channel Depth (m)	7.5	6.2	1.1	1.1	16.3	1.4
Mean Slope Angle	0.065	0.137	0.016	0.113	0.130	0.026
Sinuosity	1.2	1.3	2.1	2.0	1.3	1.5
Number of Stations	15		14		22	
Cave Length (m)	196.7		174.9		264.3	

529

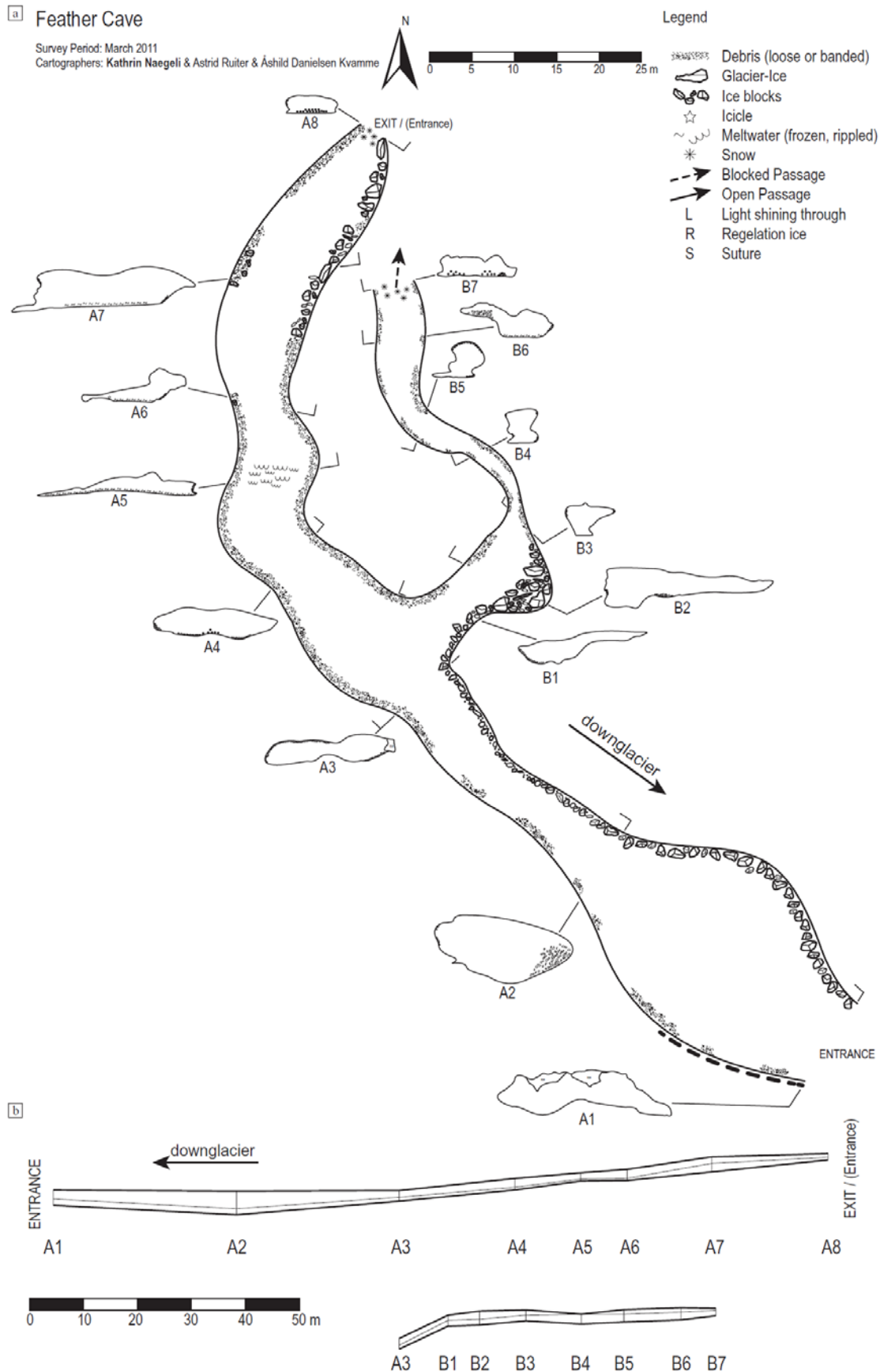
530 **Fig. 1.** Location maps: (a) Map of the Svalbard archipelago with the location of Tellbreen marked as red square. (b) 2001  
 531 Landsat ETM+ image showing location of Tellbreen (TLB) relative to Longyearbyen, Adventdalen and Helvetiadalen. (c) 2009  
 532 NPI aerial photograph of Tellbreen lower tongue. Light yellow lines show location and orientation of the four investigated  
 533 conduit systems, named Crack cave, Feather cave, Steam cave and Moulin; dots mark the entrance of each system. Feather  
 534 cave and Crack cave are located within the debris covered dead ice topography.



535  
 536  
 537  
 538  
 539  
 540

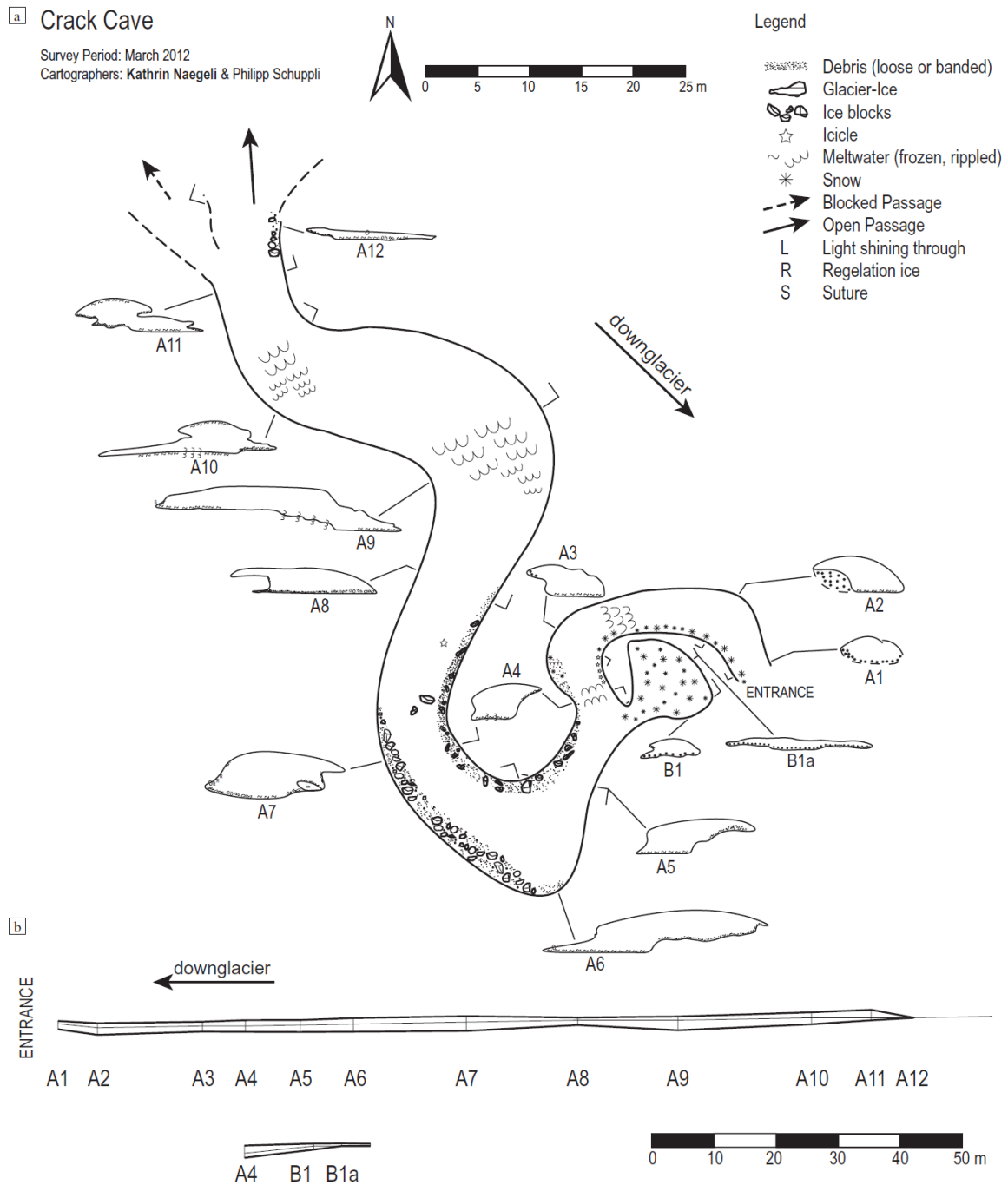


541 **Fig. 2.** Feather cave maps: (a) Plan-view map. Dashed line on the left-hand side of the entrance cavern indicates the location  
 542 of the sediments logged in Fig. 7. (b) Profile-view map showing the two separate branches of the conduit system. Cross-sections  
 543 are drawn at double the size of the plan-view scale. To see all details, especially in the cross-sections, please zoom in.



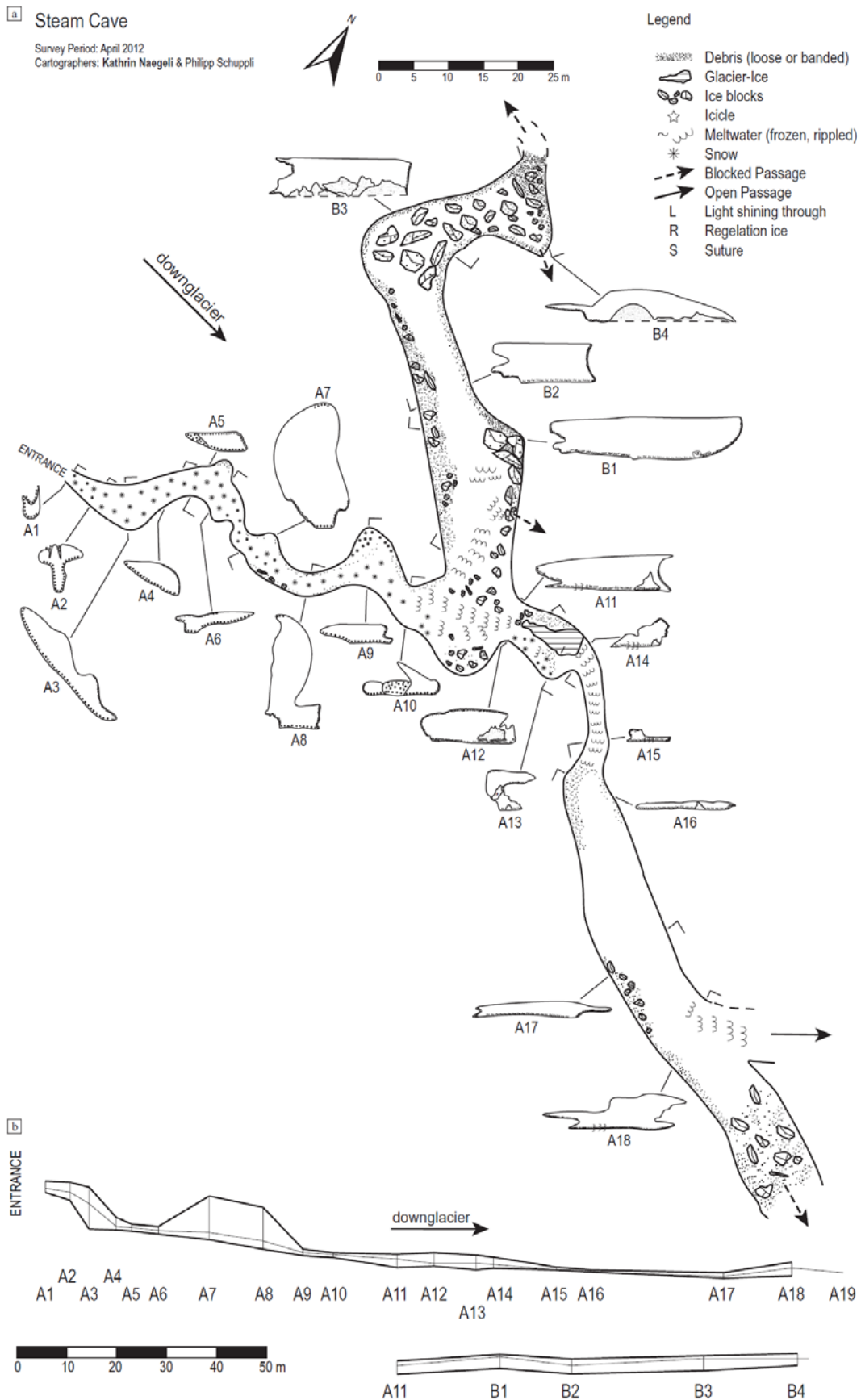
544

545 **Fig. 3.** Crack Cave maps: (a) Plan-view map. (b) Profile-view map showing the two separate branches of the conduit system.  
 546 Cross-sections are drawn at double the size of the plan-view scale. To see all details, especially in the cross-sections, please  
 547 zoom in.

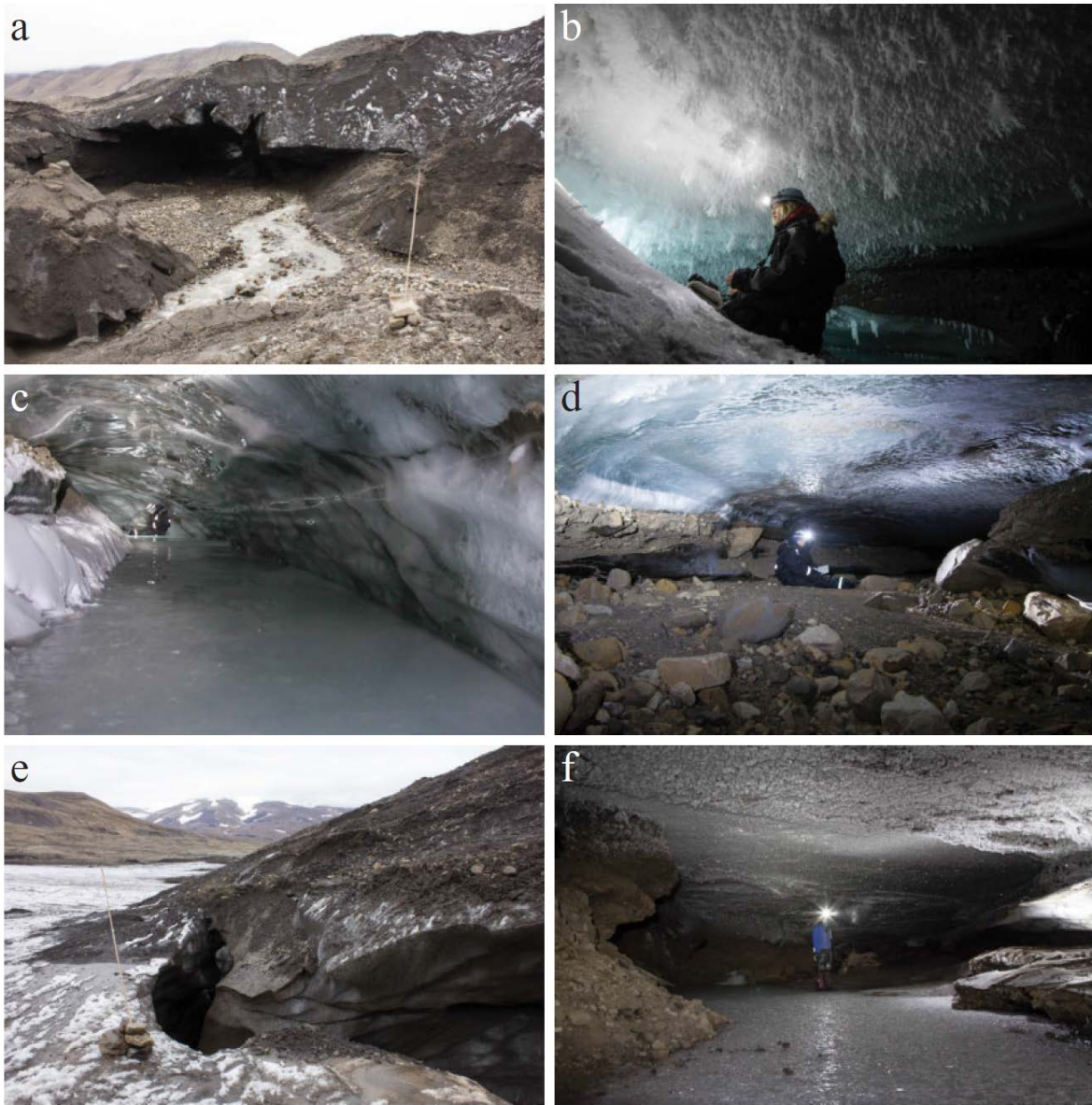


548  
 549  
 550  
 551  
 552  
 553

554 **Fig. 4.** Steam Cave maps: (a) Plan-view map. (b) Profile-view map showing the two separate branches of the conduit system.  
 555 Cross-sections are drawn at double the size of the plan-view scale. To see all details, especially in the cross-sections, please  
 556 zoom in.



558 **Fig. 5.** (a) Feather cave entrance in August 2011. (b) Ice feathers covering the roof of Feather cave. (c) Tubular channel  
 559 morphology between station A2 and A3 of Crack Cave. (d) Horizontal slot passage with floor covered by loose sediment and  
 560 rocks in Crack cave at station A8. (e) Steam cave entrance in August 2011. (f) Horizontal slot morphology between B2 and B3  
 561 of Steam cave. (g) Large N-channel cut down into the poorly-sorted diamict below the moulin. (h) Small R-channel incised  
 562 upwards into the ice at the lowest end of the moulin system. (i) N-channel extending downglacier from the moulin with the two  
 563 ice walls squeezed together due to ice flow (sutureline). (j) Channel B of Feather cave with infilled sediment band in the wall  
 564 between station B5 and B6. View is looking down channel. (k) Debris-filled sutures between station A6 and A7 of Crack cave.  
 565 (Photos taken by K. Naegeli, Ph. Schuppli and E. Welty).

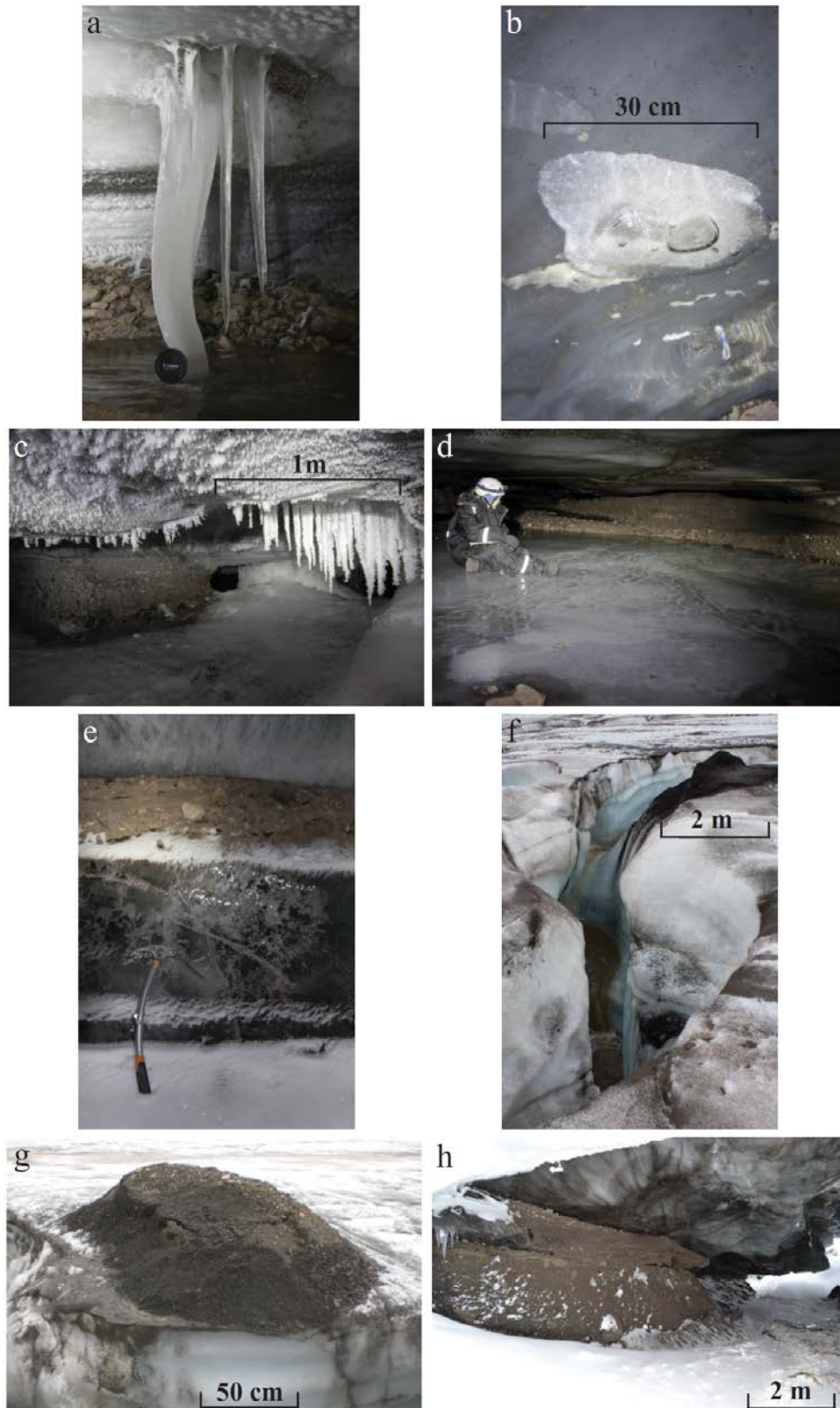


566  
 567  
 568  
 569  
 570  
 571



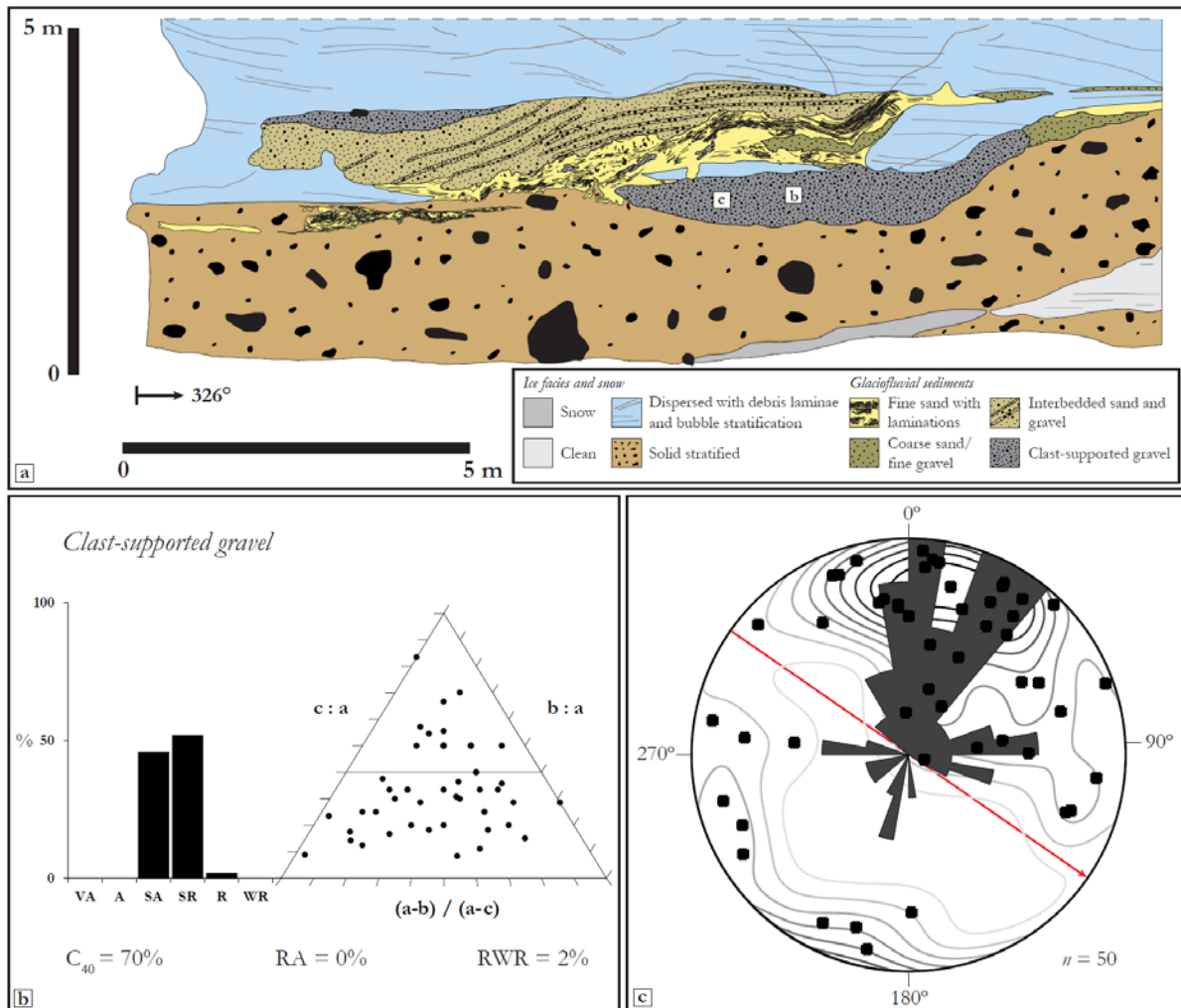
573  
574  
575  
576  
577  
578  
579  
580  
581  
582  
583

584 **Fig. 6.** Glaciological and sedimentological features found in and around the conduit systems: (a) Deformed icicle within Crack  
 585 cave between station A7 and A8. (b) Disk-like bubble structure within Crack cave between station A2 and A3. (c) Icicles at  
 586 station A10 in Steam cave. (d) Ripple structures within the cave floor of Crack cave at station A9. (e) Englacial band of sand  
 587 and gravel within Crack cave. (f) and (g) Supraglacial piles of sand and fine gravel located adjacent to a meltwater channel. (h)  
 588 Entrance of Feather cave and the englacial sediment band logged in Fig. 7. (Photos taken by H. Lovell, K. Naegeli and Ph.  
 589 Schuppli).



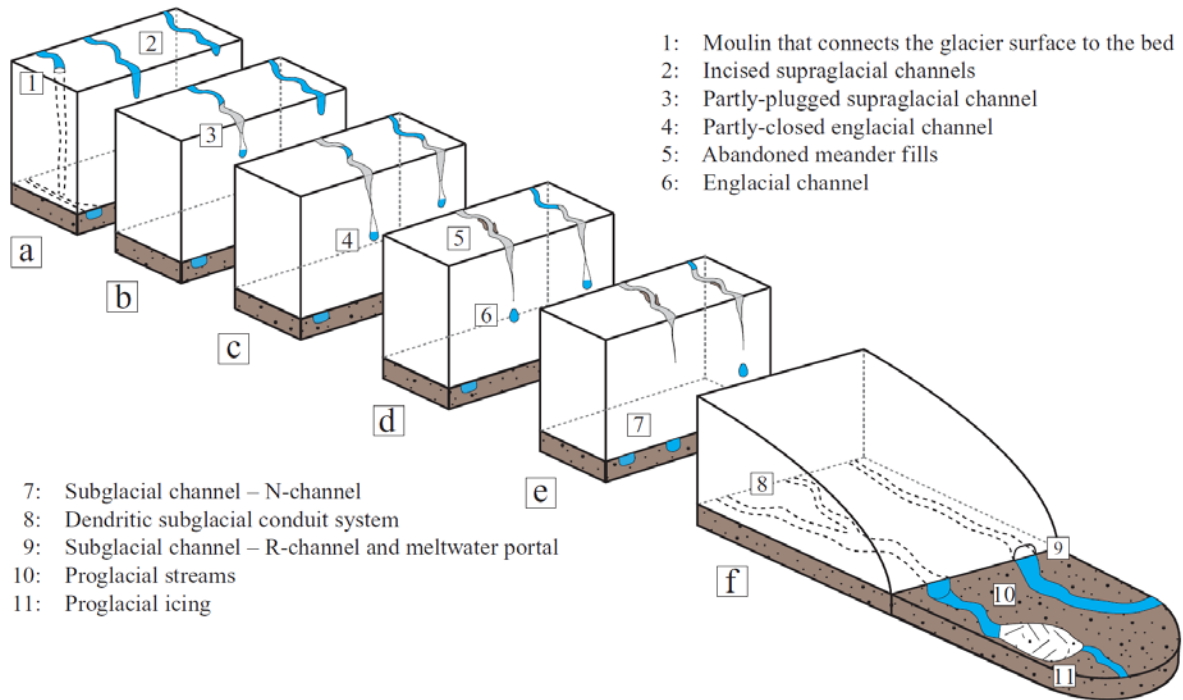
590

591 **Fig. 7.** (a) Log of sediments exposed in the wall of Feather cave (cf. Figs 1c and 2a for location). (b) Clast shape (histogram)  
 592 and roundness (ternary diagram) data for clast-supported gravel layer (VA = very angular, A = angular, SA = sub-angular, SR  
 593 = sub-rounded, R = rounded, WR = well-rounded; a, b and c = long, intermediate and short orthogonal axes of each particle  
 594 respectively). (c) Lower hemisphere equal-area stereographic projection and rose diagram of clast fabric data taken from clast-  
 595 supported gravel layer. Red arrow indicates ice flow direction. Sample locations are marked on (a).



596  
 597  
 598  
 599  
 600  
 601  
 602  
 603  
 604  
 605  
 606  
 607

608 **Fig. 8.** Conceptual diagram of the temporal and spatial evolution (stage a to f) of the drainage system within cold valley glaciers.  
 609 For more explanation please see text.



610